

Development and Evaluation of Maize Husks (Asbestos-Free) Based Brake Pad

Nuhu A. Ademoh

Department of Mechanical Engineering, Federal University of Technology, P. M. B. 65, Minna, Nigeria
E-Mail: nuhuadam@yahoo.com

Adeyemi I. Olabisi

Department of Mechanical Engineering, Federal University of Petroleum Resources, Effurum-Warri, Nigeria
Email: adeyemi.olabisi@fupre.edu.ng

Abstract

The development and evaluation of maize husks as asbestos-free friction material for the production of automotive brake pad was carried out in this work. Asbestos friction material that has been used for over 80 years was found to be carcinogenic in nature and has prompted several research efforts for its replacement from brake pads. Three sets of composite compositions were made using maize husks as filler material to impart friction properties with varied epoxy resin contents as the matrix that bonded the particles in the mix. Brake pad specimens were made out of the composites and subjected to mechanical, physical and tribological analyses to ascertain their possible performance in service using standard test procedures, materials and equipment. The particulate size of the MH filler material was 300 μ m and epoxy resin was in slurry. The result showed that specimen composite 3 with 30% MH filler content having coefficient of friction, abrasion resistance, water absorption, oil absorption, density, hardness, tensile strength, compressive strength, and thermal conductivity of 0.37, 4.470E-6g/m, 0.725%, 0.660%, 0.852g/cm³, 99.34mPa, 14.407mPa, 6.779mPa and 0.330W/mk respectively was optimum in performance. It was observed that reducing the filler content increased hardness, wear rate, tensile strength, compressive strength and thermal conductivity of the composite brake pad, while density, coefficient of friction water and oil absorption got increased with increased MH filler content. The result when compared with those of conventional brake pad made of asbestos and other friction materials of past researches showed that MH particles are an effective replacement for asbestos in automotive brake pad manufacture. Unlike asbestos based brake pad, the composite brake pads are eco-friendly and do not have the health hazards like cancer aggravation, asbestosis, mesothelioma, lung and other ailments associated with use of asbestos bearing components.

Keywords: Brake pad; asbestos; maize husks, tribological properties.

1.0 INTRODUCTION

Automotive brake lining materials which date back to 117 years ago are usually made with blends of asbestos, metals and ceramics. The asbestos constituent has been found to release gases hazardous to human health upon use of brake pads. Asbestos in any domestic components like water pipelines etc. have long been known to cause or aggravate diseases like asbestosis, mesothelioma, lung and other cancers (Anon, 2004). Consequently numerous researches have been on to discover human friendly material replacements for asbestos portions in engineering components. Asbestos as a constituent in brake lining pad composites imparts desired high friction property that automotive pads require to function properly as motion stoppers. Brake pads are important components of braking system for all categories of vehicles equipped with brake discs. They are steel backing plates with friction materials bonded unto the surface facing the brake disc and are placed in the wheel assembly to continuously clamp and hold wheels to slow them down or completely stop their motion (Aigbodion et al., 2010). Brake pads are of two types used automobile brakes. Brake shoes are located inside a drum for drum brake type so that on application of brakes, the brake shoe is forced outward and pressed against the drum. Disc brakes operate in similar way except that while drum brakes are enclosed disc brakes are exposed to environment (Bono et al., 2010). By the arrangements, particulate materials that gradually wear from brake pads are carried away by breeze into surrounding especially those from disc brakes. Most worn particles from drum brakes are retained within enclosed drums and inhaled by mechanics when they open up wheels for maintenance and repairs and gradually poison the human system.

Brake pads generally consist of asbestos fibers embedded in polymeric matrix along with some other ingredients. Use of asbestos fibres is no longer acceptable because of its carcinogenic nature leading to development of new asbestos-free friction materials for brake pads. In 1925 British Belting and Asbestos (BBA) Limited known as BBA Group manufactured well-known friction materials branded as Mintex, Don and Textar used with chrysotile asbestos in brake pads due to their effectiveness (Deepika et al., 2013). However studies conducted in 1989 by National Institutes of Health published a report that showed a high population of brake mechanics were afflicted with pleural and peritoneal mesothelioma which were linked to chrysotile and asbestos

exposure. Public health authorities made a widespread recommendation against inhaling brake dust. Since then use of chrysotile carrying pads has been restricted in many countries and it is being progressively replaced in most brake pads by fibers like synthetic aramids. In 1930s, Ferodo changed to thermosetting resins and produced molded instead of knitted linings. Molded linings were made by combining fiber with resin and polymerizing resin under elevated pressure and temperature (Deepika et al., 2013). Blau (2001) reported additive effects of different non-asbestos materials on friction lining; the result of which sensitized increased utilization of asbestos-free organic, semi-metallic and metallic friction lining materials. Non-asbestos organic (NAO) based friction materials are multi ingredient systems that contain over 10 ingredients intermixed to achieve different expected combinations of performance properties. Although, use of asbestos in brake pads has not been banned all over the world, many brake pad industries are moving away from it use because of concerns regarding airborne particles in factories and disposal of wastes containing asbestos. Several patents for asbestos free organic friction materials exist (Dagwa, 2005) with more than 700 items classified into four categories consisting of binder, fiber, friction modifiers and fillers based on the major functions apart from controlling friction and wear resistance.

According to Kim et al. (2003) class A organic disc brake pads were first adopted to make the switch from four wheels drum brake to disc front-drum rear systems. They were made from asbestos and effective for low temperatures. As cars started to get smaller in late 1970's, it became harder to cool brake pads and class B organic pads that worked better at higher temperature were developed though, they were also found to have certain problems including durability (Mathur et al., 2004; Dagwa and Ibadode, 2005). Changes in brake pad formulations were also driven by corporate promulgations of average fuel efficiency requirements in late 1970's and mid 1980's which led automobile industry to switch from rear wheel drive cars to front wheel drive cars. This switch required more front braking that generated higher temperature and preference for semi-metallic brakes (Gudmand-Hoyer et al., 1999). Consequently, many studies have been done and are still ongoing for development of not only asbestos-free brakes but also less temperature generating pads for better human health and technical efficiency. Coconut and palm kernel shells (PKS) were used successfully to replace asbestos in brake pad materials (Dagwa, 2005; Aigbodion and Akadike, 2010). Bashar et al (2012) and Deepika et al (2013) showed that palm kernel shells (PKS) gave good friction material for brake pads and that PKS is cheap biomass that is readily obtainable from agro wastes as characterized by Ishidi et al. (2011).

Bashar et al (2012) formulated brake pad with multi-composite including ground coconut shell filler; epoxy resin binder matrix, iron chips reinforcement, methyl ethyl ketone peroxide catalyst, cobalt naphthanate accelerator, iron with silica abrasive and brass as friction modifier. It showed that higher percentage coconut shell powder gave lower breaking, hardness, compressive and impact strengths; implying that increased coconut powder increased brittleness of pads. This agreed with the result of Ishidi et al (2011) that tensile/impact strength of treated and untreated palm kernel shell reinforced polymer composite decreased with increased filler content. Yawas et al (2013) used periwinkle shell as asbestos substitute in brake pad that contained phenolic resin, SEA 20/50 engine oil and water.

Aderiye (2014) characterized beneficiated kaolin for automotive friction lining material production and concluded that the clay group has good potentials for use due to its good heat resistance. Idris et al (2013) produced brake pads using banana peel to replace asbestos and phenol formaldehyde binder varied from 5-30% at interval of 5%. Result showed that compressive strength, hardness and specific gravity of samples increased with increased resin; while oil and water soak; wear rate and percentage charred decreased with increased resin. Egg shell based eco-friendly brake pads was developed and evaluated by Edokpia et al (2014) with gum Arabic binder varied from 3-18%. Wear rate, thickness swelling in water/oil, thermal resistance, specific gravity, compressive strength, hardness and micro-structural test results showed that samples with 18% gum Arabic gave optimum performances that compared favourably with commercial brake pads and that temperature of maximal decomposition was higher than asbestos and most agro-biomass based brake pads. This review showed that global researches today are mostly focused on ways of using agro-biomass; hitherto incinerated as unuseful wastes into eco-friendly bio-degenerable and sustainable sources of industrial raw materials.

It is based on these potentials of bio-mass usage that this project was conceived to use maize husks (MH) as base friction material for production of eco-friendly automotive brake pads free of asbestos. Previous study revealed that MH is lingo-cellulosic with composite structure constituted by organic matrix reinforced with bundles of cellulose micro-fibres. Its organic matrix is mostly composed of lignin, hemicellulose, pectin, wax and protein. The chemical and fibre compositions are as presented in tables 1 and 2 (Taiwo et al., 2014). The coefficient of friction of maize husk was determined as 0.5 at density of 45-80lb/ft³ (Nazire, 2013); making it a good candidate for friction material particularly in brake lining applications. The mechanical characterization of maize husk by Guimarães et al (2008) is presented in table 3. The aim of this work therefore, is to formulate reliable automotive brake pads from composites based on maize husk friction material. The main objectives are to develop some asbestos free brake pads from composite formulation using maize husk as the friction material; test samples of the developed brake pads for performance evaluations including abrasion resistance, hardness, friction coefficient, tensile/compressive strengths, specific gravity, oil/water absorptions, stopping time, thermal

conductivity and disc temperature as adopted by Dagwa and Ibadode (2005) and to compare the result with qualities of commercial and laboratory brake pads produced with asbestos and other friction materials. The significance of this work when successfully completed will lie in the facts that it will contribute a part solution to the health dangers of asbestos base brake pads in general and particularly move Nigeria a step forward towards the actualization of her local content initiative of the use of locally made products in indigenous automotive industry.

Table 1: Chemical composition of maize husk

| Component | Amount (%) |
|--|------------|
| Lignin | 15 |
| Ash | 5.09 |
| Alcohol-cyclohexane solubility (1:2 v/v) | 4.57 |
| Cellulose | 44.08 |

Table 2: Characteristics of maize husk

| Fibre property | Dimension |
|-----------------------------|-----------|
| Fibre length (mm) L | 1.71±0.5 |
| Fibre diameter (µm) D | 21.89±5.1 |
| Cell wall thickness (µm) CW | 7.63±2.3 |
| Lumen width (µm) LW | 6.63±3.5 |

Table 3: Mechanical properties of maize husk.

| Mechanical Properties | Longitudinal | | Transversal | |
|------------------------|--------------|--------------------|-------------|--------------------|
| | Mean | Standard Deviation | Mean | Standard Deviation |
| Tensile Strength (MPa) | 10.8 | 4.32 | 4.2 | 2.35 |
| Elastic Modulus (MPa) | 387.4 | 141.7 | 169.3 | 81.0 |
| Rupture Strain (%) | 5.03 | 1.02 | 3.7 | 1.4 |

2.0 RESEARCH MATERIALS AND METHODS

The experimental brake pads were developed from carefully selected materials as advised by Blau (2001) following standard production procedure as described by Edokpia et al (2014) and Bashar et al (2012) and then evaluated with the standard test methods adopted by Dagwa and Ibadode (2005).

2.1 Research Materials and equipment

The materials used for this work included maize husks (obtained from a maize farm centre after corn seed was shelled from cub), silica sand, epoxy resin, calcium carbonate, anhydrous iron oxide, talc as release agent and powdered graphite. Laboratory equipment included sieve of aperture 300µm (BS 410-1), steel spatula, stirrer, bowls, LCD series 2-digit/3-digit electronic weigh balances, aluminum moulds, scrapper, hand gloves, universal testing machine (model-INSTRON-3369), micro hardness machine (model-LECO-LM700AT), metal files, Taber abrasion tester (TST-instrument-TSE-A016), measure rule, inclined plane, water, SAE60 automotive engine oil and modified Lee's disc apparatus. The functions and needs for each material are as described in table 4. Apart from maize husks, other chemical material inputs into the experimental specimens were purchased from standard chemical dealer's shop in Ibadan, Nigeria. The laboratory and workshop equipments were accessed at Engineering materials Development Institute, Akure, Nigeria. Other equipments were used at Federal University of petroleum Resources, effurum and Federal University of Technology, Minna, Nigeria.

Table 4: Functions of selected experimental Materials

| S/N | Materials | Role | Function in composite |
|-----|--|-------------------|--|
| 1. | Epoxy resin and Hardener | Matrix/binder | To explore its suitability as binding agent in brake pad, as it is not commonly used. |
| 2. | Maize husk | Filler | Cheaply available as waste in farm lands. Literature shows it has properties that favour its use in friction lining manufacture. |
| 3. | Silica iron oxide | Abrasive | Easy and cheap to obtain. It is useful for increasing friction and controlling the build-up of friction film. |
| 4. | Calcium carbonate (CaCO ₃) | Reinforcement | It is the cheaper alternative to barites. It influences adhesion and disperses polymer in composites. |
| 5. | Powdered graphite | Friction Modifier | It is not hazardous for improving wet friction. |

2.2 Research Methods

The experimental work of the study was conducted in the following stages

2.2.1 Raw material preparation:- The base raw material, maize husk (MH) was collected from a farm centre, properly sun-dried on screed surface, and cleaned to remove impurities. It was thereafter crushed in hammer mill and ground into powder as shown in (figure 1a) and then sieved using a sieve of 300 μ m aperture to obtain finely divided powder as in (figure 1b). Other experimental chemicals were classified and contained in well labeled transparent glass containers for easy identification.



Figure 1: Photograph of raw maize husks: (a) Crushed husk; (b) Sieved powdered husk

2.2.1 Specimen brake pad production:-The technique of powder metallurgy as practiced by Edokpia et al (2014) and Bashar et al (2012) was adopted and used for producing test brake pad specimens for fixing pre-cast mixture onto the surface of the backing steel metal plates. A control test was initially performed by pouring 250g of epoxy resin into moulds to determine the exact amount of mixture that would completely fill the cavity. The weight of maize husk filler material (MH), matrix (epoxy resin hardener) was varied while that of the abrasives (silica and iron oxide), friction modifier (pulverized graphite), and reinforcement (calcium carbonate – CaCO₃) was kept constant. For each formulation quantities expressed in percentage weight presented in table 5 for fillers, abrasives, friction modifier and reinforcement were measured into mixing vessel and thoroughly mixed for 15 minutes to obtain homogeneity. The desired amounts of epoxy resin (polyepoxide) as shown in table 5 was poured into a separate container and required quantity of hardener was added to form the matrix and thoroughly stirred for about 10 minutes to obtain uniform mixture. Thereafter, the matrix mixture was poured onto the powdered friction material mixture and stirred further to obtain a paste-like homogenous mixture. The formed paste was poured into mould cavities that already had powdered talc applied for ease of component removal after casting and allowed to cure for 80 to 120 minutes. Resistance to flow of paste was observed to decrease as weight of matrix binder increased as curing period varied depending on the ratio of epoxy resin to hardener in mixture. The ratio of epoxy resin to hardener constituents of mixture was 1:2 for composition 1 and 1:3 for compositions 2 and 3.

Table 5: Material formulation for the MH based brake pads

| S/N | Material | Composition 1 (%) | Composition 2 (%) | Composition 3 (%) |
|-----|------------------------|-------------------|-------------------|-------------------|
| 1. | Epoxy resin + Hardener | 50.0 | 55.0 | 60.0 |
| 2. | CaCO ₃ | 4.0 | 4.0 | 4.0 |
| 3. | Maize husk powder | 31.0 | 26.0 | 21.0 |
| 4. | (a) Silica | 7.0 | 7.0 | 7.0 |
| | (b) Iron oxide | 3.0 | 3.0 | 3.0 |
| 5. | Powdered Graphite | 5.0 | 5.0 | 5.0 |
| | Total | 100.0 | 100.0 | 100.0 |

The same process was repeated to produce other brake pad samples and experimental test specimens. A selection of some of the test specimens after casting and curing are as presented in figure 2 for the abrasion, tensile and thermal conductivity analyses. The specimens were kept in well aerated environment for 21 days for attainment of full strength before carrying out the analytical tests. Cease et al (2006) and Simpson (2014) kept specimens for 7 days strengthening before mechanical tests. The specimens were collected and classified after strengthening days and subjected to tests that included coefficient of friction, wear (abrasion) resistance, water/oil absorption, density, thermal conductivity, hardness, tensile and compressive strengths as practiced by Edokpia et al (2014); Hooton (1969); Deepika et al (2013) and Dagwa (2005) to ascertain suitability of formulation for friction application.

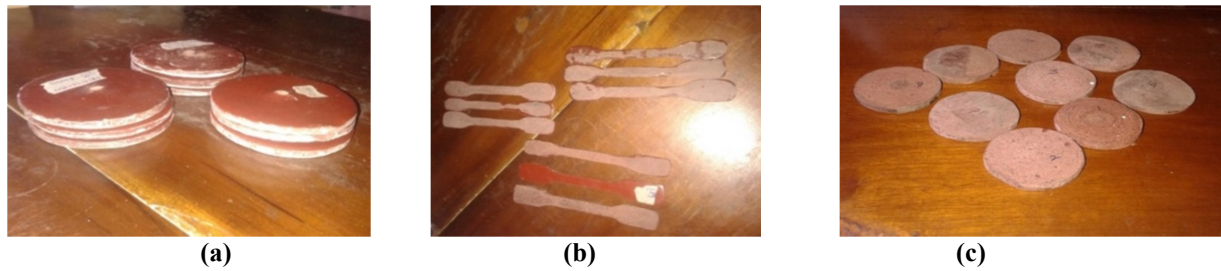


Figure 5:-Selected samples of brake pad formulation test specimens as produced: (a) Abrasion test samples; (b) Tensile strength test samples; (c) Thermal conductivity test samples.

2.2.2 Specimen brake pad test analyses:-Each group of specimens was subjected to standard tests to determine the empirical values of the essential brake pad analytical parameters. .

(a) Coefficient of friction test:-Each specimen was placed on inclined plane of known angle and a 90° wedge as illustrated in figure 3. Wedge position was varied to increase angle until specimen was just about to slide down plane. Equation 1 was used to calculate resulting coefficient of static friction (μ).

$$\mu = \tan \theta = \frac{\text{opp.}}{\text{adj.}} \dots\dots\dots(1); (\text{www.pstcc.edu, 2005})$$

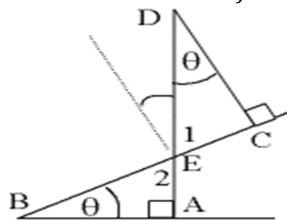


Figure 2:-Illustration of specimen for coefficient of static friction test

(b) Abrasion resistance test:-Each wear/abrasion resistance specimen measured 110mm in diameter by 6mm thickness as shown in figure 3. Test was conducted with taber abrasion (TST instrument – model TSE-A016). Each specimen was weighed and recorded as W_0 before test using FA2204B 4-digit electronic weigh balance. Specimen was fixed to a 100mm diameter rotary disc of machine with the aid of a nut in its centre. Two emery wheels at the upper arm of the machine were allowed to have direct contact with the specimen fastened to the rotary disc. The machine was powered on (at 220V) and disc rotated at constant speed of 85revs/min for pre-set time of 1000 seconds. As the disc rotated, the two emery wheels in direct contact with the specimen also rotated at a relative speed to disc and caused specimen to wear. After the pre-set time, machine was turned off automatically. The specimen was thoroughly cleaned and the final weight measured and recorded as W_1 . Weight loss in specimen was determined by difference between final and initial weight (ie. $W_1 - W_0$) from which the wear rate was calculated using equation 2 (Bashar et al., 2012 and Edokpia et al., 2014).

$$\text{Wear Rate} = \frac{w_0 - w_1}{s} = \frac{\Delta W}{S} = \frac{\Delta W}{2\pi ND \times t} \dots\dots\dots(2)$$

Where: W_0 = initial weight; W_1 = final weight; ΔW = weight loss; S = sliding distance; D = disc diameter; N = radial speed (rpm) and t= time taken to expose specimen to wear.

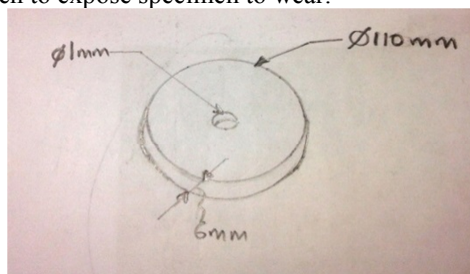


Figure 3:-Schematic diagram of abrasion test specimen

(c) Oil and Water soaking tests:-Initial weight of each specimen was taken and recorded as W_0 before soaking in SAE60 auto engine oil and distilled water separately for 48 hours as in figure 4. After, specimens were brought out of oil and water, thoroughly cleaned to remove water and oil on surfaces, reweighed and recorded as W_1 . Differences in initial and final weights for each specimen were then used to determine absorption rate in accordance with Edokpia et al (2014) using 3.

$$Absorption (\%) = \left(\frac{W_1 - W_0}{W_0} \right) \times 100 \dots\dots\dots (3)$$

Where: W_0 =weight of specimen before immersion; and W_1 = weight of specimen after immersion.

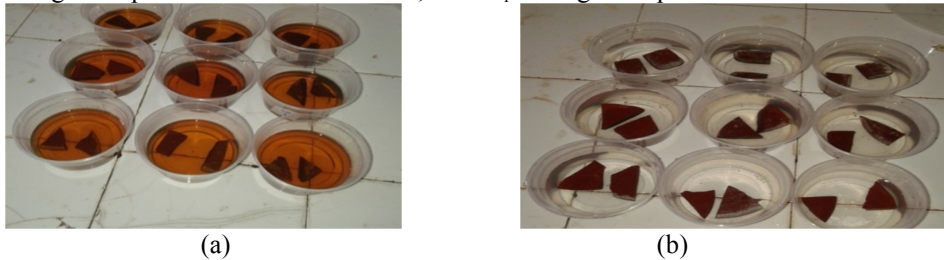


Figure 4:-Absorption test specimens soaked in (a) SAE60 automotive oil; (b) Distilled water.

(d) Density test:-Density test was conducted on experimental brake pad using Archimedes’ principle as practiced Edokpia et al (2014) for determining volume and thus, density of an irregularly shaped object by measuring its mass in air and effective mass when submerged in water (density = 1 g/cc).

(f) Hardness test Oil:-A digital micro hardness tester of 490.3μN load sensitivity (model: LECO LM700AT) was used to measure specimen hardness. Each specimen was indented for 10 seconds (d well time), after which corresponding Vickers’s hardness number was read directly from the counter.

(g) Tensile strength tests:-Electronic universal testing machine (Model: INSTRON 3369) was used to determine specimen tensile strength. Average specimen gauge length, width and thickness measured 85 by 11 by 6mm respectively as in figure 5. One end of specimen was gripped in jaws attached to adjustable crosshead and after lifting this crosshead to appropriate height; the other end of specimen was fixed in jaws of top crosshead. Tensile load was hydraulically applied by pressing start bottom in the control unit. The input and output display unit in control unit indicated the magnitude of applied load. The load was gradually increased until specimen broke off and the corresponding extension was noted and recorded. The test data generated was automatically shown on the display unit.

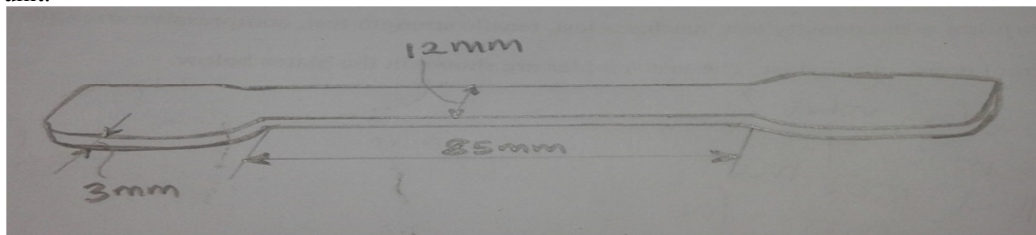


Figure 5: Schematic diagram of tensile test specimen

(h) Compression test:-The same universal strength machine (Model: INSTRON 3369) was used to measure compressive strength. Specimens were cuboid in shape and dimensioned as 40 × 12×6mm as in figure 6. A specimen was placed between the compression plates provided in adjustable cross head and bottom crosshead, properly positioned and gripped. Load was then applied gradually and the corresponding compressive strain was read at regular intervals from output display unit.

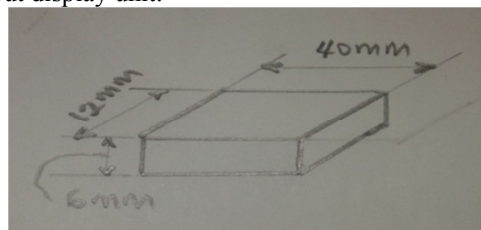


Figure 6:- Schematic diagram of compression test specimen

(i) Thermal conductivity test:-The test was conducted with modified Lee’s disc apparatus on brake pad specimen as adopted by Oluyamo et al (2012). The setup included a power source, a rheostat, an ammeter, a voltmeter and four thermometers that measured temperatures of the 3 discs as T_A , T_B , T_C and surrounding ambient temperature, T_{Amb} respectively. The experiment was conducted in enclosed environment to minimize heat loss to surrounding. The brass discs were 4.14cm in diameter with hole drilled at the edge to a depth to accommodate thermometer. Inside each hole was poured glycerine for proper contact. A heater was kept between discs B and C to maintain their thermal equilibrium. A test piece which of 41mm diameter by 5mm thickness as in figure 7 was placed between discs A and B in contact with each other. To the start test for rising temperature readings, the rheostat was set to adjust voltage to maximum of 6V and after every 5 minutes temperature rise was read until equilibrium was attained. This was repeated six times consecutively and thereafter, rheostat was reset to reduce both voltage

and current to make temperature fall. Falling temperature was also read at 5 minutes interval until equilibrium was attained. The thermal conductivity (λ W/mk) result for specimen of thickness (t -mm) and radius (r -mm) was computed with the equations below. A MATLAB programme developed by Oluyamo et al (2012) was used to compute thermal conductivity at different time intervals.

$$\lambda = \frac{ed}{2\pi r^2(T_B - T_A)} \left[a_s \frac{T_A + T_B}{2} + 2a_A T_A \right] \dots\dots\dots(4)$$

Where e is given as; $e = \frac{VI}{[a_A T_A + a_s \frac{T_A + T_B}{2} + a_A T_B + a_C T]}$ (5) and

$$a_A = a_C = \pi r^2 + 2\pi r l_d \dots\dots\dots(6)$$

$$a_B = 2\pi r l_d \dots\dots\dots(7)$$

$$a_s = 2\pi r l_s \dots\dots\dots(8)$$

Where l_d and l_s were disc and sample thicknesses; a_A , a_B , a_C and a_s were the exposed surface areas of discs A, B, C and specimen respectively. T_A , T_B and T_C were temperatures of discs A, B and C above ambient (i.e. thermal equilibrium temperature of disc minus ambient temperature). V and I were potential differences across the heater and current which flowed through it respectively.

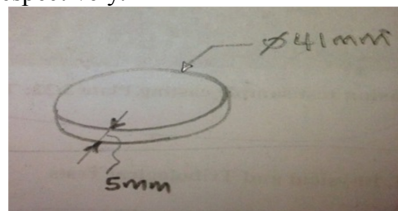


Figure 7:- Schematic diagram of thermal conductivity test specimen

3. RESULTS AND DISCUSSION

Table 6 presents the results of 3 tests and the average on coefficients of friction of specimens for each of the three experimental brake pad compositions with the parameters used during the tests.

Table 6: Coefficient of friction (μ) of specimens.

| Test No | Sample group Description | Adj. (cm) | Opp. (cm) | Angle (θ°) | Average (θ°) | Friction coefficient (μ) For; $\mu = \tan\theta$ | Average μ |
|---------|--------------------------|-----------|-----------|--------------------------|----------------------------|--|---------------|
| 1. | Composition 1 | 22.20 | 10.70 | 25.73 | 23.69 | 0.48 | 0.44 |
| 2. | | 24.70 | 10.70 | 23.42 | | 0.43 | |
| 3. | | 26.60 | 10.70 | 21.91 | | 0.40 | |
| 1. | Composition 2 | 26.80 | 10.70 | 21.76 | 21.62 | 0.40 | 0.40 |
| 2. | | 27.50 | 10.70 | 21.26 | | 0.39 | |
| 3. | | 26.70 | 10.70 | 21.84 | | 0.40 | |
| 1. | Composition 3 | 28.50 | 10.70 | 20.58 | 20.13 | 0.38 | 0.37 |
| 2. | | 29.20 | 10.70 | 20.12 | | 0.37 | |
| 3. | | 29.90 | 10.70 | 19.69 | | 0.36 | |

The coefficient of friction was used to plot graph presented in figure 8 against the experimental brake pad compositions and that of commercial (conventional brake pad) and results were inter-compared.

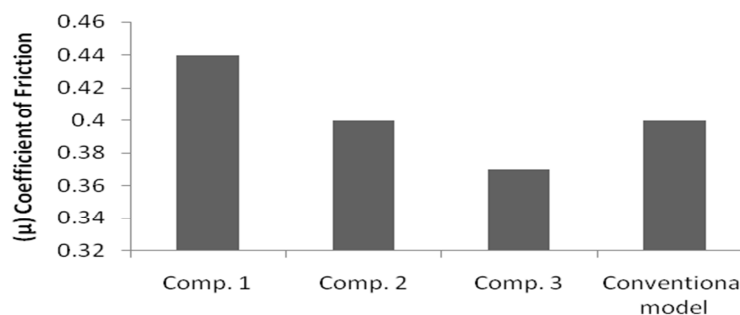


Figure 8:-Coefficient of friction (μ) of different specimen composition

In figure 8, coefficient of friction decreased as filler content of mix decreased in each composition. The coefficient of friction of each sample composition compares favourably with that of conventional brake pad obtained from a standard (Hooton, 1969). The value for brake pad composition 1 with 31% maize husk was the highest with friction coefficient of 0.44; composition 1 had 0.40 and composition 3 had 0.37. The coefficient of

friction of any conventional brake pad is usually in the range 0.3 - 0.4 (Ibhadode and Dagwa, 2008). This implied that all the three formulations satisfy the requirement with composition 1 excelling above the range. By comparison, friction coefficient of composite specimens 1, 2 and 3 varied above the mean values of that of commercial brake pad (0.35.) by 25.71%, 14.29% and 5.71% respectively. Friction coefficient of specimen composition 1 with 50% binder was higher than those obtained in related works by Ibhadode and Dagwa (2008) that used conventional filler; Aigbodion et al (2010) that used bagasse filler; Edokpia et al (2014) that used egg shell filler and Yawas et al (2013) that used periwinkle filler for composite brake pads with variances of 0.09, 0.02, 0.14 and 0.06 respectively while it agreed with value (0.44) obtained by Dagwa and Ibhadode (2005). Result of wear rate tests of composite brake pad specimen with test parameters is presented in table 7. Three sets of tests were conducted for each specimen composition and the average value determined. The was determined as: $Wear Rate = \frac{w_o - w_1}{s} = \frac{\Delta W}{S} = \frac{\Delta W}{2\pi ND \times t}$; N = 85rev/min; D=0.1m; t = 1000secs.

Table 7: Wear Rate and test parameters of composite brake pad specimens.

| Test No | Sample group Description | W _o (g) | W ₁ (g) | Time (sec.) | ΔW (g) | Average ΔW (g) | Wear Rate ×10 ⁻⁶ (g/m) |
|---------|--------------------------|--------------------|--------------------|-------------|--------|----------------|-----------------------------------|
| 1. | Sample Composition 1 | 102.649 | 102.635 | 1000 | 0.014 | 0.017 | 3.040 |
| 2. | | 103.921 | 103.907 | 1000 | 0.014 | | |
| 3. | | 105.233 | 105.211 | 1000 | 0.022 | | |
| 1. | Sample Composition 2 | 103.141 | 103.121 | 1000 | 0.020 | 0.023 | 4.112 |
| 2. | | 107.057 | 107.034 | 1000 | 0.023 | | |
| 3. | | 107.037 | 107.012 | 1000 | 0.025 | | |
| 1. | Sample Composition 3 | 101.382 | 101.361 | 1000 | 0.021 | 0.025 | 4.470 |
| 2. | | 100.990 | 100.966 | 1000 | 0.024 | | |
| 3. | | 91.079 | 91.050 | 1000 | 0.0290 | | |

The wear rates were plotted against composite brake pad compositions and commercial brake pad for close comparison as in figure 9 which shows that wear rate of experimental brake pads increased as epoxy resin content increased from 50 to 60%. This is because maize husk acted both as friction and abrasion resistant material in the composite; so increase in epoxy resin meant reduction in filler and abrasion resistant material that resulted to higher wear. However, the wear rates compare closely with that of conventional brake pads that has wear rate of 3.80×10^{-6} g/m (Ibhadode and Dagwa, 2008).

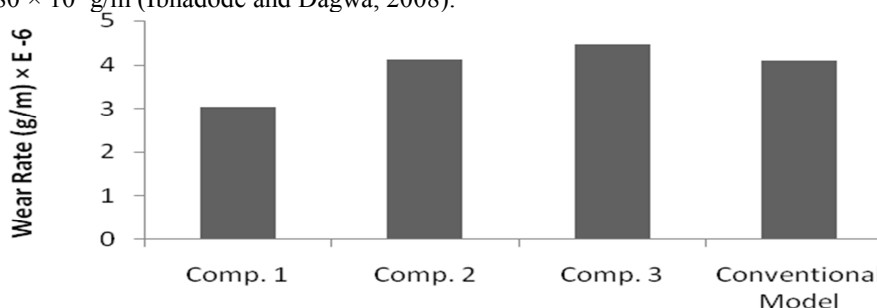


Figure 9:- Wear rate analysis of specimens

The wear rates of the composite brake pad compositions 1, 2 and 3 differed from that of conventional brake pad by -0.760, 0.312 and 0.67 respectively; making composite 1 with 50% binder) a superior brake pad material to the conventional brake pad. In comparison with previous works composition 1 was better than the brake pad made with conventional material (Ibhadode and Dagwa, 2008); bagasse filler (Aigbodion et al., 2010); egg shell filler (Edokpia et al., 2014) and periwinkle filler (Yawas et al., 2013) with variances of 43.52%, 51.23%, 48.90% and 46.35% respectively.

Table 8 presents average water and oil absorption test results for the 3 formulated composite brake pads. The table shows initial weights before specimen immersion in oil/water; average weight gain and percentage absorption of oil/water. Figure 10 is a bar chart of percentage absorption of oil/water per composite pad composition. Absorption was computed as $Absorption (\%) = \frac{\Delta W_{avg.}}{W_{o(avg.)}} \times 100$.

Table 8: Water and Oil absorption (%) of composite brake pads.

| Sample group description | Water | | | Oil | | |
|--------------------------|--|---|----------------|--|---|----------------|
| | Ave. Initial Weight, $W_{o(avg.)}$ (g) | Ave. Weight gain, $\Delta W_{avg.}$ (g) | Absorption (%) | Ave. Initial Weight, $W_{o(avg.)}$ (g) | Ave. Weight gain, $\Delta W_{avg.}$ (g) | Absorption (%) |
| Composition 1 | 4.015 | 0.055 | 1.370 | 2.570 | 0.025 | 0.973 |
| Composition 2 | 5.210 | 0.060 | 1.152 | 3.915 | 0.030 | 0.766 |
| Composition 3 | 6.210 | 0.045 | 0.725 | 3.030 | 0.020 | 0.660 |

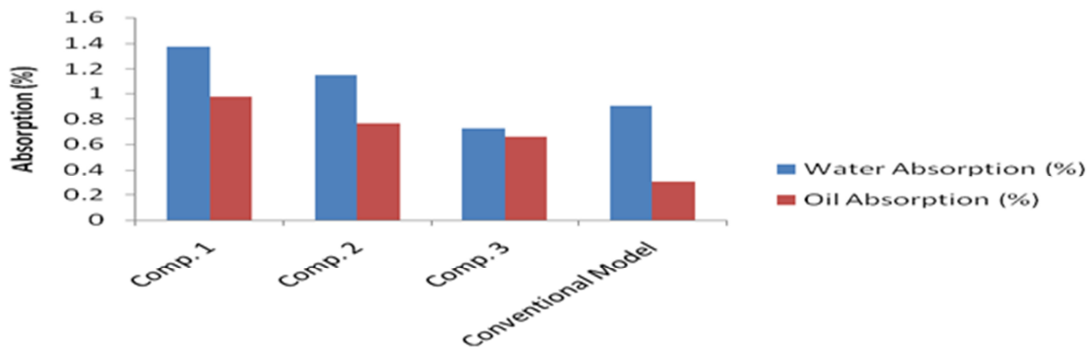


Figure 10:- Water and oil absorption analysis of the samples

In figure 10, water absorbent property of samples decreased as weight of fillers decreased from 31% to 21% in the formulation. Oil absorption of samples decreased order as filler content decreased from 31% to 21% in formulation. This decreased water and oil absorption rate may be due to the increased interfacial bonding between binder and filler particle that caused decreased porosity (Edokpia *et al.*, 2014). The result compared favourably with that of conventional model with water and oil absorption rates of 0.9% and 0.3% respectively. Water absorption rate of each composite deviated from that of conventional brake pad by 0.470 (composition 1), 0.252 (composition 2) and -0.175 (composition 3). Oil absorption rate of composites 1, 2 and 3 deviated from that of commercial brake pads by 0.673, 0.466 and 0.360 respectively. Negative variance indicated that water and oil absorption of composite was lower than that of conventional model showing its superiority over the latter. Thus, composition 3 with 60% binder gave least absorption rate making it better than the conventional brake pad of Ibadode and Dagwa (2008), palm kernel shell based brake pad of Dagwa and Ibadode (2005), bagasse based brake pad of Aigbodion *et al* (2010) and egg shells based brake pad of Edokpia *et al* (2014). The variance of water absorption rates of this work from results of these previous works were 0.175, 4.305, 2.755 and 2.485 respectively while oil absorption rates were -0.360, -0.220, 0.450 and 0.490 respectively. This implied composite pad produced in the work had better water/oil absorption than conventional model and will offer better resistance on exposure to environmental water vapour and oil on application. Result of density test on 3 experimental compositions is presented in table 9.

Table 9: Density and test parameters of experimental maize husks based brake pads

| Test No | Sample group description | Weight in air W_{air} (g) | Water displaced V (cm ³) | Aver. Weight in air, $W_{air(avg.)}$ (g) | Aver. Vol. of water displaced $V_{avg.}$ (cm ³) | Average Density $\rho_{avg.}$ (g/cm ³) |
|---------|--------------------------|-----------------------------|--|--|---|--|
| 1 | Composition 1 | 3.750 | 3.970 | 4.015 | 4.165 | 0.964 |
| 2 | | 4.280 | 4.360 | | | |
| 1 | Composition 2 | 6.560 | 8.010 | 5.210 | 6.240 | 0.835 |
| 2 | | 3.860 | 4.470 | | | |
| 1 | Composition 3 | 5.420 | 6.290 | 6.210 | 7.286 | 0.852 |
| 2 | | 7.000 | 8.282 | | | |

The density results were extracted and plotted against the compositions of specimens as presented in figure 11 where density varied irregularly with decreasing filler content. This is indicative of specific gravity of specimens. The increase was attributable to increased packing of filler particle that formed better homogeneity in composite brake pads (Edokpia *et al.*, 2014). The weight/density of specimens was less than that of commercial brake pad (1.890g/cm³) but conform to standard (Hooton 1969).

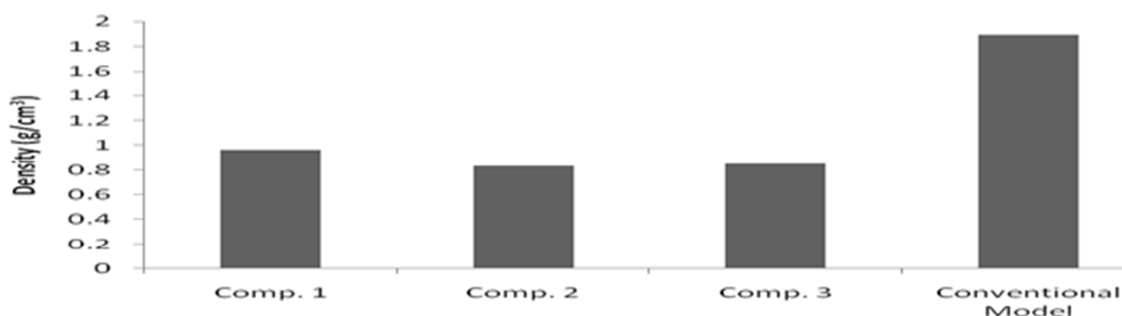


Figure 17: Density versus composite brake specimen compositions

The density of each composite specimen compositions 1, 2 and 3 varied from that of the conventional brake pad by 43.99%, 55.82% and 54.92% respectively. Lower density indicated better quality than a standard conventional brake pad (Edokpia et al., 2014). Result of hardness test on experimental brake pad is in table 10 where hardness was plotted and compared with conventional brake pad (figure 11).

Table 10: Hardness (Vickers) value of composite brake pads

| S/N | Sample group description | Hardness Number (HV) | Average Hardness Number (HV) | Average Hardness Value (MPa) |
|-----|--------------------------|----------------------|------------------------------|------------------------------|
| 1 | composition 1 | 9.80 | 9.90 | 97.09 |
| 2 | | 9.40 | | |
| 3 | | 10.50 | | |
| 1 | composition 2 | 8.60 | 8.57 | 84.05 |
| 2 | | 8.40 | | |
| 3 | | 8.70 | | |
| 1 | composition 3 | 10.70 | 10.13 | 99.34 |
| 2 | | 9.40 | | |
| 3 | | 10.30 | | |

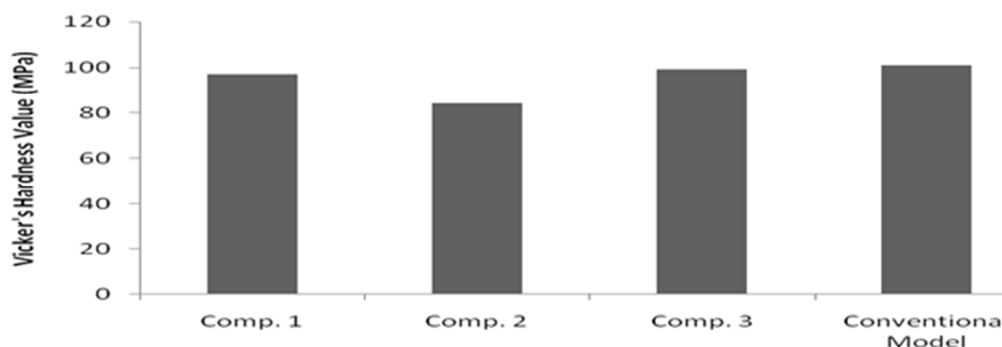


Figure 11: Comparison of Vickers hardness of composite brake pad specimens

The figure showed that hardness of composite brake pads varied non-uniformly with increased epoxy resin in formulation. Values compared with but varied from conventional model by 3.91%, 15.78% and 1.54% for composite compositions 1, 2 and 3 respectively. The high hardness is attributable to the increase in bonding and close packing that strain hardened the composite brake pad and raised its hardness. Hardness composite brake pads compared with those of conventional brake pad (101MPa) and results of other related studies. The high specimen hardness accounted for high wear rates and frequency of regrinding the HSS tool steel used for its plane turning and facing on lathe machine. Table 11 presents the result of 3 sets of tensile strength tests on each composite brake pad specimen.

Table 11: Average tensile strength of composite pads

| Sample group description | Aver tensile stress at break (MPa) | Aver tensile strain at break (mm/mm) | Average Modulus (MPa) | Average Load at break (N) | Average Extension at break (m) |
|--------------------------|------------------------------------|--------------------------------------|-----------------------|---------------------------|--------------------------------|
| Composition 1 | 10.675 | 0.047 | 610.290 | 532.356 | 0.005 |
| Composition 2 | 12.671 | 0.050 | 459.504 | 764.028 | 0.004 |
| Composition 3 | 14.407 | 0.068 | 370.349 | 564.960 | 0.070 |

The result showed decreasing filler content from 31 to 21% caused increased tensile strength. A pillar drilling machine (RIGI DRILL DP-25) was used to bore holes at the centre of abrasive test specimen. The chips generated as presented in figure 12 had a nature that indicated ductility of the materials.



Figure 12: Chips generated by face turning specimen on lathe machine

Tensile strength presented in figure 13 for each composite specimen reasonably compared with that of conventional brake pad. The brittleness of composite brake pad got increased with filler content in the formulation. The load (N) to extension (mm) relationship at break point is as presented in figure 14. The load/extension graph showed that filler/binder content has significant effect on tensile load required to produce specific extension before rupture as indicative of specimen plasticity.

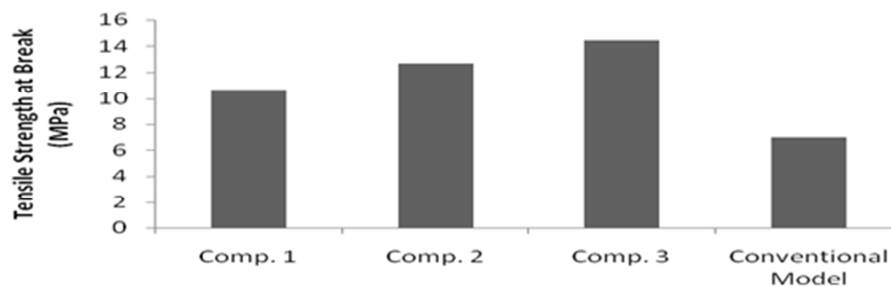


Figure 13: Comparative analysis of tensile strength of composite pads.

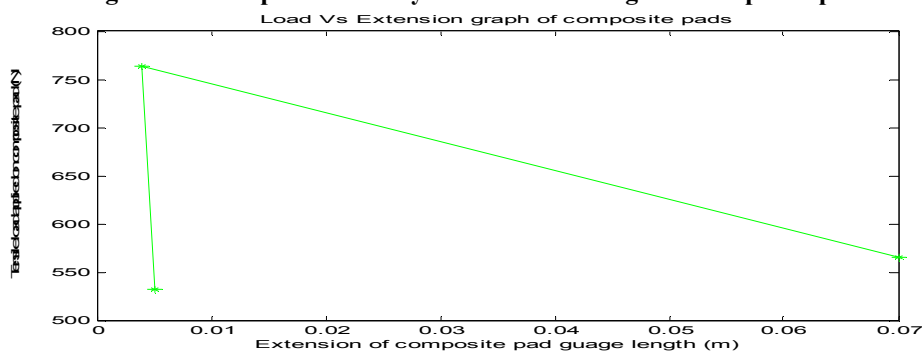


Figure 14: Load VS Extension graph for the composite pads

Tensile strength of specimen deviated positively from that of conventional brake pad (7.00MPa) by 53.57% 81.00% and 105.86% for compositions 1, 2 and 3 respectively. The values are higher than those produced in previous related studies summarized in table 14. The result of compressive strength of pad is in table 12.

Table 12: Compressive strength of composite pads

| Description | Comp. Stress (mPa) | Strain (mm/mm) | Modulus (mPa) | Break load (N) |
|---------------|--------------------|----------------|---------------|----------------|
| Composition 1 | (-) 3.965 | 0.012 | 330.373 | (-) 200.322 |
| Composition 2 | (-) 5.501 | 0.014 | 390.118 | (-) 280.149 |
| Composition 3 | (-) 6.779 | 0.016 | 415.883 | (-) 320.466 |

The negative signs in some values of table 12 (in brackets) showed that no specimens broke under the applied load implying that it is only loads that are much higher than the test loads can rupture them. Figure 15 was developed from compressive test data to compare the performances of the composites.

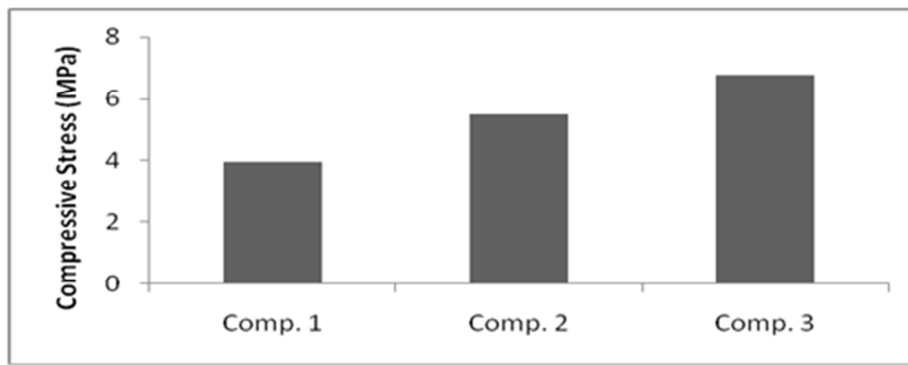


Figure 15: Comparison of compressive strength of the composite brake pads.

Result in figure 15 followed similar trend with that of hardness test such that compressive strength increased with increased epoxy resin content. This accounted for fair dispersion of MH filler particles with binder leading to proper filler particle/binder interaction that increased ability of the formulated composite brake pad to resist gross deformation as explained by Edokpia et al (2014). In figure 16, a steady increase in stress-strain occurred with decreased percentage of filler in specimens. Composite pad with 60% binder gave the highest compressive strength and stress-strain values because increase in pore packaging ability of filler particle in matrix. Decreased compressive strength with decreased epoxy resin was caused by the interference of particles in the mobility or deformability of the matrix. This interference was created through the physical interaction and immobilization of the binder by the presence of mechanical restraints, thereby reducing strength as explained by Edokpia et al (2014).

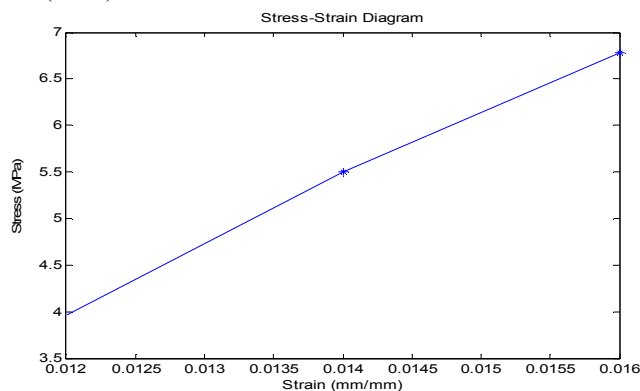


Figure 16: Stress-strain diagram of the composite brake pad specimens

Table 13 presents thermal conductivity results of the tested specimens of newly developed brake pad. It showed that specimen thermal conductivity decreased with increased MH filler in composite because of the lower interfacial bonding between filler particles and decreased matrix content.

Table 13: Thermal conductivity of composite brake pad.

| Composition | Thickness (mm) | Diameter (mm) | Thermal Conductivity (λ W/mk) |
|---------------|----------------|---------------|--|
| Composition 1 | 5.30 | 40.10 | 0.1776 |
| Composition 2 | 5.80 | 38.60 | 0.2331 |
| Composition 3 | 5.50 | 40.00 | 0.3300 |

The thermal conductivity of each of the experimental composite brake pad and that of conventional brake pad were plotted into the graph presented in figure 17 for easy assessment and intercomparison.

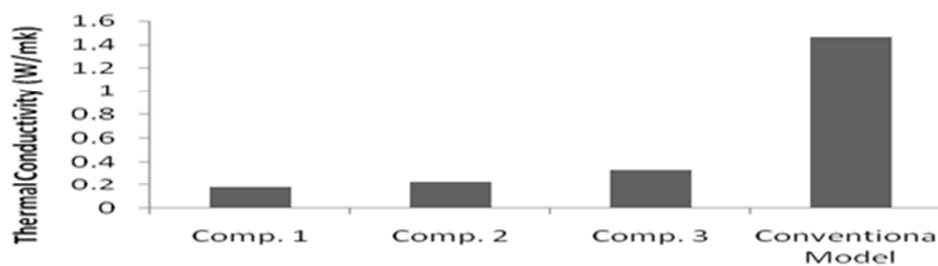


Figure 17: Comparative analysis of the thermal conductivity of composite brake pads

Figure 17 showed that thermal conductivity of each of the composite brake pad was far below that of conventional brake pad (0.539W/mK) implying that the composite pads have better heat resistance than conventional model. Information on thermal conductivity was not readily available on previous studies on agro-waste based brake pads except that on palm kernel shell based brake pad developed by Dagwa and Ibadode (2005) that gave a value of 1.460W/mK. Composition 3 (with 21% filler) displayed the highest thermal resistivity. It varied from that of the conventional brake pad by 38.48%.

A general summary on results of this study showing how each of the parameters and properties of brake pad specimens inter-compared with each other; with results of past works by other authors and with conventional/commercial brake pads are as presented in table 14.

Table 14: Summary of results compared with the existing laboratory brake pads

| Properties | Asbestos based commercial brake pad | Palm kernel shell based pad | Bagasse based brake pad | Egg Shell particles at 18% of GA | Periwinkle shell based brake pad at 125µm | (PKS+CBS+MH at 300µm) |
|---|-------------------------------------|-----------------------------|-------------------------|----------------------------------|---|-----------------------|
| Spec. gravity (g/cm ³) | 1.890 | 1.650 | 1.430 | 1.650 | 1.010 | 0.853 |
| Wear rate (mg/m) | 3.800 | 4.400 | 4.200 | 4.000 | - | 2.146 |
| Friction Coefficient | 0.30 – 0.40 | 0.44 | 0.42 | 0.30 | 0.35 – 0.41 | 0.37 – 0.40 |
| Thickness swell in H ₂ O (%) | 0.9 | 5.03 | 3.48 | 3.21 | 0.39 | 0.91 |
| Thickness swell in SAE oil (%) | 0.30 | 0.44 | 1.11 | 1.15 | 0.37 | 0.58 |
| Hardness Values (MPa) | 101.0 | 92.0 | 100.5 | 99.1 | 116.7 | 127.8 |
| Compressive strength (MPa) | 110.0 | 103.5 | 105.6 | 103.0 | 147.0 | 10.3+ |
| Tensile strength (MPa) | 7.00 | 6.80 | - | - | - | 20.22 |
| Thermal conduct. (W/mK) | 0.539 | 1.460 | - | - | - | 0.251 - 0.372 |

In table 14 the curing time of composites changed from 80 minutes for 1:2 ratio of hardener to epoxy resin in the mixture to 120 minutes for 1:3 ratio of hardener to epoxy resin in the composite. Also, during the experimental specimen production it was generally observed that changing the matrix mix ratio from 1:2 to 1:3 reduced porosity observed with the casting.

4.0 CONCLUSIONS

Results obtained from experimental aspects of this work that determined properties like coefficient of friction, abrasion resistance, water absorption, oil absorption, density, hardness, tensile strength, compressive strength, and thermal conductivity each of three compositions of maize husk filler based brake pads compared favourably with commercial brake pads and those produced in past related research works on asbestos free brake pads. The work showed that reducing filler content increased hardness, wear rate, tensile strength, compressive strength and thermal conductivity of the composite brake pads; while density, coefficient of friction water absorption and oil absorption increased with increased filler content. Based on the results maize husks are a very suitable eco-friendly replacement for asbestos and many agro-biomass friction materials in automotive brake pads.

ACKNOWLEDGEMENT

The authors of this work hereby acknowledge the laboratory assistance offered by Dr. Oladele of Metallurgical and Materials Engineering Department and that of Mr. Bello, Physics Department both of Federal University of Technology, Akure, Nigeria.

References

- Aderiyeye (2014). Kaolin Mineral Material for Automobile Ceramic Brake Pad Manufacturing Industry: International Journal of Technology Enhancements and Emerging Engineering Research, Vol. 2, Issue 3. ISSN 2347-4289.
- Anon (2004). Automotive brake repair trends and safety issues: <http://www.sirim.my/amtee/pm/brake.html>
- Aigbodion, V. S., Akadike, U., Hassan, S. B., Asuke, F., Agunsoye, J. O. (2010). Development of Asbestos – free Brake Pad Using Bagasse. Tribol. Ind. 32 (1), 45–50.

- Aigbodion, V. S., Agunsoye, J. O. (2010). Bagasse (Sugarcane waste): Non-Asbestos Free Brake Pad Materials. LAP Lambert Academic Publishing, Germany, ISBN 978-3-8433-8194-9.
- Bashar, Dan-Asabe, Peter, Madakson B., Joseph, Manji (2012). Material Selection and Production of a Cold-worked Composite Brake Pad. World Journal of Engineering and Pure and Applied Science (WJEPAS). 2(3):96.
- Bono, S. G., Dekyrger, W. J. (1990). Auto Technology, Theory and Service, 2nd ed. DELMAR Publishers, New York, 45–48.
- Blau, J. P. (2001). Compositions, Functions and Testing of Friction Brake Materials and their Additives. Being a report by Oak Ridge National Laboratory for U.S. Dept. of Energy. <http://www.Ornl.gov/webworks/cppr/y2001/rpt/112956.pdf>, 78–80.
- Cease, H., Derwent, P. F., Diehl, H. T., Fast, J., Finley, D. (2006). Measurement of mechanical properties of three epoxy adhesives at cryogenic temperatures for CCD construction: Fermi National Accelerator Laboratory. Batavia IL 60510.
- Chief Agri/Industrial Division (2013), Kearney, United States, NE 68848: Apparent Densities of Dry Feed Ingredients.
- Dagwa, I. M., Ibadode, A. O. A. (2005). Design and Manufacture of Automobile Disk Brake Pad Test Rig: Nigerian Journal of Engineering Research and Development, Vol. 4 (3), pp.15 - 24.
- Dagwa, I. M. (2005). Development of Automobile Disk Brake Pad from Local Materials, Ph.D. (Manufacturing Engineering) Thesis, University of Benin, Benin City, Nigeria.
- Dagwa, I. M., Ibadode, A. O. A. (2006). Determination of Optimum Manufacturing Conditions for Asbestos-free Brake Pad Using Taguchi Method: Nigerian Journal of Engineering Research and Development. Basade Publishing Press Ondo, Nigeria, pp. 1–8, 5(4).
- Deepika, K., Bhaskar, Reddy C., Ramana, Reddy D. (2013). Fabrication and Performance Evaluation of a Composite Material for Wear Resistance Application. International Journal of Engineering Science and Innovative Technology (IJESIT) Volume 2, Issue 6.
- Edokpia, R. O., Aigbodion, V. S., Obiorah, O. B., Atuanya, C. U. (2014). Evaluation of the Properties of Ecofriendly Brake Pad Using Egg Shell Particles–Gum Arabic. ScienceDirect®, Elsevier B.V. DOI: 10.1016/j.rinp.2014.06.003
- Gudmand-Hoyer, L., Bach, A., Nielsen, G. T., Morgen, P. (1999). Tribological Properties of Automotive Disc Brakes with Solid Lubricants. Wear 232, 168–175.
- Guimarães, G. M., Paes, M. C. D., França, F., Marconcini, J. M. (2008). Corn Husks Mechanical Characterization. marconcini@cnpdia.embrapa.br
- Hooton, N. A. (1969). Metal-Ceramic Composites in High-Energy Friction Applications: *Bendix Technical Journal*, Spring 1969, pp. 55-61. (Concerning aircraft brakes)
- Ishidi, E. Y., Kolawole, E. G., Sunmonu, K. O. (2011). Morphology and thermal property of alkaline treated palm kernel nut shell HDPE composite. Journal of Emerging Trends in Engineering and Applied Sciences (JETEAS);2(2):346-350
- Khurmi, R. S. and Gupta, J. K. (2004): A Text Book of Workshop Technology (Manufacturing Processes). S. Chand & Company Ltd. Reprinted edition. Page 58 – 67
- Kim, S. J., Kim, K. S., Jang, H. (2003). Optimization of manufacturing parameters for brake lining using taguchi method. J. Mater. Process. Technol. 136, 202–208.
- Mathur, R. B., Thiyagarajan, P., Dhama, T. L. (2004). Controlling the Hardness and Tribological Behavior of Non-asbestos Brake Lining Materials for Automobiles. J. Carbon Sci. 5 (1), 6–11.
- Nazire, Deniz Yilmaz (2013). Effects of enzymatic treatments on the mechanical properties of corn husk fibres, The Journal of the Textile Institute, Vol. 104, No. 4.
- Oluyamo, S. S., Bello, O. R., and Yomade, O. J. (2012). Thermal Conductivity of Three Different Wood Products of Combretaceae Family; *Terminalia superba*, *Terminalia ivorensis* and *Quisqualis indica*. Journal of Natural Sciences Research. Vol. 2, No. 9.
- Simpson Strong-Tie (2014): flexiblized Epoxy Adhesive. FX-523
- Sivarao, M., Amarnath, M. S., Rizal, A. K. (2009). An investigation toward development of economical brake lining wear alert system, IJENS, Vol: 9, No.9, pp. 251-256.
- Taiwo, K. Fabemigun, Fagbemi, O. D., Otitoju, O., Mgbachiuzor, E., Igwe, C. C. (2014). Pulp and paper-making potential of corn husk. International Journal of AgriScience. Vol. 4(4): 209 – 213
- Yawas, D. S., Aku, S. Y., Amaren, S. G. (2013). Morphology and properties of periwinkle shell asbestos-free brake pad. Journal of King Saud University – Engineering Sciences.
- www.ptcc.edu/departments/natural_behavioral_sciences/Web%20Physics/Experiment%2005.htm

The IISTE is a pioneer in the Open-Access hosting service and academic event management. The aim of the firm is Accelerating Global Knowledge Sharing.

More information about the firm can be found on the homepage:

<http://www.iiste.org>

CALL FOR JOURNAL PAPERS

There are more than 30 peer-reviewed academic journals hosted under the hosting platform.

Prospective authors of journals can find the submission instruction on the following page: <http://www.iiste.org/journals/> All the journals articles are available online to the readers all over the world without financial, legal, or technical barriers other than those inseparable from gaining access to the internet itself. Paper version of the journals is also available upon request of readers and authors.

MORE RESOURCES

Book publication information: <http://www.iiste.org/book/>

Academic conference: <http://www.iiste.org/conference/upcoming-conferences-call-for-paper/>

IISTE Knowledge Sharing Partners

EBSCO, Index Copernicus, Ulrich's Periodicals Directory, JournalTOCS, PKP Open Archives Harvester, Bielefeld Academic Search Engine, Elektronische Zeitschriftenbibliothek EZB, Open J-Gate, OCLC WorldCat, Universe Digital Library, NewJour, Google Scholar

